

# Alternating seismic uplift and subsidence in the late Holocene at Madang, Papua New Guinea: Evidence from raised reefs

Alexander W. Tudhope,<sup>1,2</sup> Robert W. Buddemeier,<sup>3,4</sup> Colin P. Chilcott,<sup>1</sup> Kelvin R. Berryman,<sup>5</sup> Daphne G. Fautin,<sup>6,7</sup> Matthew Jebb,<sup>8,9</sup> Jere H. Lipps,<sup>10</sup> Robert G. Pearce,<sup>1</sup> Terence P. Scoffin,<sup>1</sup> and Graham B. Shimmield<sup>11</sup>

**Abstract.** Well-preserved mid-late Holocene coral reefs are exposed in low coastal cliffs in the vicinity of the Madang lagoon on the north coast of Papua New Guinea. Results from U/Th and <sup>14</sup>C dating of corals, surveying, and field mapping indicate several major changes in relative sea level over this period. Specifically, there is evidence for a relative sea level fall of  $\geq 4.5$  m about 3000 calendar years B.P., followed by relative sea level rises of  $\sim 1.5$  m about 2400 calendar years B.P. and  $\geq 0.5$  m about 1200 calendar years B.P. and a subsequent relative sea level fall of  $\geq 3$  m some time in the past 1000 years. Since regional eustatic sea levels are believed to have been dropping gradually over this time frame, these observed changes in relative sea level are interpreted as reflecting alternating tectonic uplift and subsidence. Furthermore, the detailed structure and age relationships of the coral deposits indicate that both uplift and subsidence occurred rapidly, most probably as coseismic events with vertical displacements of 0.5 to 4.5 m. These events may be related to rupture on NW-SE trending reverse faults which have been mapped in the nearby Adelbert Range and possibly on NE trending cross faults which have been inferred from seismicity. This interpretation implies a much greater degree of tectonic instability and potential seismic hazard in the region than previously recognized, although the inferred coseismic vertical displacements are shown to be consistent with present-day local seismicity. In a broader context, the study illustrates how detailed analysis of vertical changes in coral reef structure and assemblages may be used as a sensitive indicator of changing relative sea level, capable of resolving century timescale events and reversals.

## 1. Introduction

Analysis of the elevation and age of late Quaternary reefs may be used to glean evidence for past changes in relative sea level. These data are generally used in one of two ways. For regions and time intervals over which global (eustatic) sea level is well known the evidence from reefs may be used to determine the magnitude, sense, and timing of vertical move-

ment of the land, for example, due to coseismic events or isostatic factors [e.g., Taylor *et al.*, 1987; Ota *et al.*, 1993; Chappell *et al.*, 1996a; Zachariasen *et al.*, 1999]. Alternatively, when vertical movements of the land are well known, reefal evidence may be invoked to reconstruct eustatic sea level, for example, due to the growth and decay of high-latitude ice sheets over the late Quaternary [e.g., Chappell, 1974; Chappell and Shackleton, 1986; Chappell *et al.*, 1996b]. In this study, we adopt the first of these two approaches, presenting evidence for vertical movements of the land in the area of Madang on the north coast of Papua New Guinea over the past 3000 years. In particular, we focus on evidence for rapid and high-magnitude subsidence and uplift events in a context of relatively slow net tectonic uplift.

## 2. Regional Tectonic Setting

Northern Papua New Guinea has a complex tectonic setting due to rapid and oblique convergence of the West Pacific and Australian Plates (Figure 1). The region experiences extensive seismic and volcanic activity, and along considerable stretches of the mainland coast, net tectonic uplift has led to the subaerial exposure of Quaternary reef sequences. These raised reefs are particularly well developed on the Huon Peninsula, where average uplift rates of up to 3.5 mm/yr have prevailed for at least the past 300,000 years [Chappell, 1974].

The study area near Madang is part of the collision zone between the Finisterre Terrane and the Australian continent (see Abbott [1995] for a review). This collision began in

<sup>1</sup>Marine Geoscience Unit, Department of Geology & Geophysics, Edinburgh University, Edinburgh.

<sup>2</sup>On sabbatical at Australian Institute of Marine Science, Townsville, Queensland.

<sup>3</sup>Nuclear Chemistry Division, Lawrence Livermore National Laboratory, Livermore, California.

<sup>4</sup>Now at Kansas Geological Survey, University of Kansas, Lawrence.

<sup>5</sup>Institute of Geological and Nuclear Sciences, Lower Hutt, New Zealand.

<sup>6</sup>California Academy of Sciences, Golden Gate Park, San Francisco, California.

<sup>7</sup>Now at Department of Systematics and Ecology, University of Kansas, Lawrence.

<sup>8</sup>Christensen Research Institute, Madang, Papua New Guinea.

<sup>9</sup>Now at National Botanic Gardens, Glasnevin, Dublin.

<sup>10</sup>Museum of Paleontology and Department of Integrative Biology, University of California, Berkeley.

<sup>11</sup>Dunstaffnage Marine Laboratory, Oban, Scotland, UK

Copyright 2000 by the American Geophysical Union.

Paper number 1999JB900420.  
0148-0227/00/1999JB900420\$09.00

Miocene-Pliocene time and is ongoing. The Finisterre Terrane is composed of two distinct blocks: the Adelbert block (largely synonymous with the Adelbert Range) and the Finisterre block (largely synonymous with the Finisterre Range). These two blocks may be separated by a NE trending cross fault which runs through Astrolabe Bay (Figure 1) [Abbott *et al.*, 1994], and the change in coastline trend at Madang (to approximately N-S, in contrast to the regional WNW-ESE trend) may represent an offset of a once linear Adelbert-Finisterre block. However, marked differences in the sedimentary rock record of the two blocks [Abbott, 1995] and the lack of an equivalent offset of the Bismarck volcanic arc point to additional complexity.

Abbott [1995] suggested that collision of the Finisterre block was orthogonal with continental material on both sides, resulting in high uplift, while the collision of the Adelbert block may have been "soft" because of the presence of a trapped piece of oceanic crust between the Adelbert block and the continental margin [Milsom, 1981]. This soft collision has resulted in lower rates of uplift. For example, Miocene-age Gowop limestone is at 1600 m elevation atop the Adel-

bert Range and at 4000 m in the Finisterre Range [Robinson *et al.*, 1976; Jaques and Robinson, 1980]. Therefore vertical tectonic displacement in the study area may be influenced both by the mapped NW trending reverse faults in the Adelbert Range which trend toward the Madang lagoon and also by postulated north or NE trending cross faults such as that presumed to have ruptured during the 1970 Madang earthquake whose epicenter was in Astrolabe Bay (Figure 1), [Everingham, 1975; Abers and McCaffrey, 1994].

### 3. Field Area

The study site lies a few kilometers north of the town of Madang ( $5^{\circ}13'S$ ;  $145^{\circ}49'E$ ), in an area where the dominant ESE-WNW trend of the Papuan coastline gives way to a N-S strike and where the well-developed Madang lagoon occurs (Figure 2). This lagoon is 13 km long and 2-4 km wide, has an average midlagoon depth of 30 m, and is bounded by a living barrier reef whose top lies ~1 m below mean low water spring tide level. Tidal flushing of the lagoon waters occurs through three deep passes and over the reef crest. Spring tide

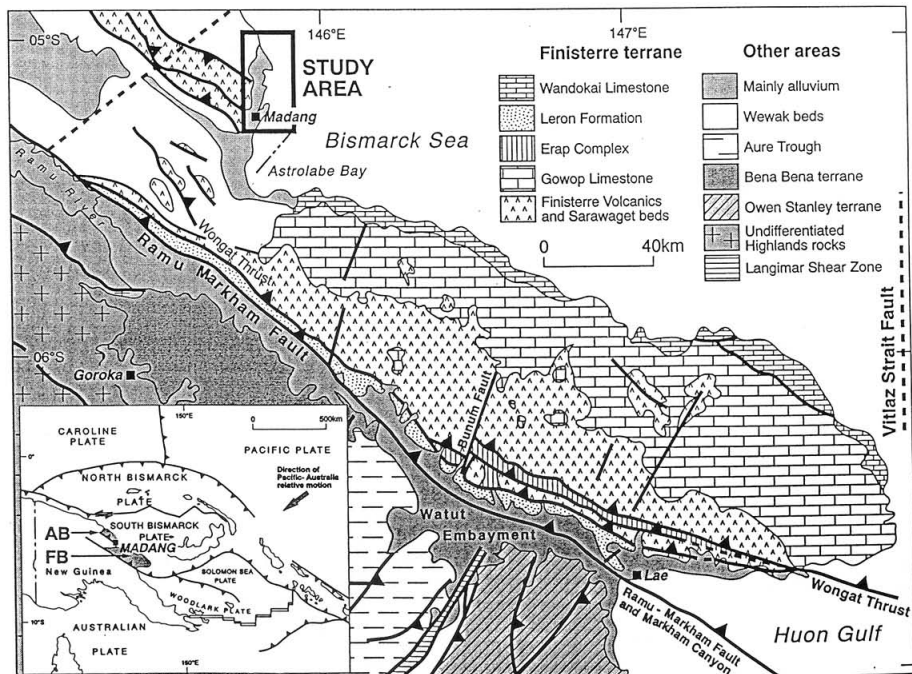


Figure 1. Tectonic setting of the study area, north coast of Papua New Guinea. In the inset, the Adelbert block and the Finisterre block of the Finisterre Terrane are shown in heavy shading and labeled with AB and FB, respectively. In the main figure (based on Abbott *et al.* [1994]), heavy solid lines are faults with barbs on the upper plate of thrusts, the NE and north trending dashed lines are seismically active strike-slip faults, and the dash-dotted line in Astrolabe Bay marks a postulated NE trending cross fault that is presumed to have ruptured during the 1970 Madang earthquake [Everingham, 1975; Abers and McCaffrey, 1994]. Inset figure is based on Tregoning *et al.* [1998].

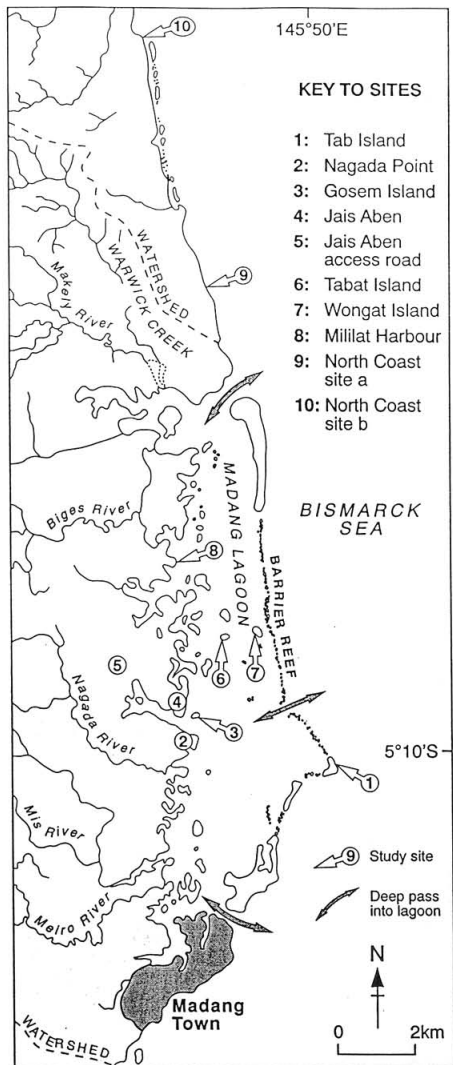


Figure 2. The Madang lagoon and surrounding area, indicating the location of sites investigated in this study.

range is  $\sim 1$  m. Within the lagoon, living reefs occur as an almost continuous fringing reef along the mainland coast and as midlagoon patch reefs that reach to within a few meters of sea level.

Well preserved Holocene raised reef deposits form a low-lying coastal plain on the mainland and form islands of up to

a few meters elevation on the outer barrier reef and on top of some midlagoon patch reefs. These deposits are particularly well exposed in an actively eroding 2-3 m high cliff which occurs along much of the mainland coast and around some islands (Figure 3). In some locations there is a second, smaller and less well exposed, cliff a few tens of meters inland which steps up a further 1-2 m. These two cliffs have been previously recognized by Panzer [1933] and by Stoddart [1972]. Throughout the rest of this paper they are referred to as the "lower coastal cliff" and "upper coastal cliff" respectively. A detailed investigation of the age, composition, and internal structure of the lower and better exposed of the two cliffs forms the focus for the present study.

Inland from the coastal cliffs is a low-lying plain with limited exposure of the underlying substrate. However, at a few localities, reef limestones outcrop at elevations ranging from a few meters up to about +80 m and at distances up to 4 km from the coast. All of the limestones above about +10 m elevation are heavily recrystallized, and consequently, they have yielded no material suitable for U/Th dating (J. Chappell, personal communication, 1999). Although the coral species composition of these more elevated limestones is indicative of a Pleistocene age, consideration of their state of preservation and karst development led Chappell (personal communication, 1999) to suggest that reefs of last-interglacial origin are absent above an elevation of about +15 m. If this assessment is correct, it implies average net tectonic uplift of less than  $\sim 0.2$  mm/yr in the late Quaternary. Farther inland, these limestones give way to the Finisterre Volcanics of Lower Oligocene to Lower Miocene age (Robinson et al., 1976).

#### 4. Materials and Methods

Holocene reef deposits exposed in the coastal cliffs and terraces were examined at six locations on the mainland coast within and north of the lagoon, on three lagoon patch reef islands, and on one barrier reef island (Figure 2). At the Jais Aben, Wongat Island, and Tab Island sites, conventional leveling techniques using a Wild automatic level were used to measure the elevation of raised reef deposits with respect to the highest living reef crest *Porites* corals. These highest living corals had a characteristic flat-topped form, with living coral tissue restricted to the outer rims and sides of the coral skeleton and a bare (dead) surface across the flat top. This flat-topped, or "microatoll" form is a result of upward restriction of coral growth by sea level such that subsequent coral growth is only in a lateral sense [Scoffin and Stoddart, 1978]. Coral microatolls can provide valuable evidence for past changes in relative sea level. For example, changes in sea level over the lifetime of an individual colony are recorded as patterns of increasing and/or decreasing elevation of the colony top, while changes over longer timescales may be deduced from comparison of the elevation of the tops of ancient (dead) colonies of different ages [Scoffin and Stoddart, 1978; Taylor et al., 1987; Zachariassen et al., 1999]. At Jais Aben the elevation of the top of the living coral microatolls was measured to be  $-0.49$  m relative to mean sea level, as defined by the Australian Commonwealth Scientific and Industrial Research Organisation (CSIRO) for the nearby tide gauge. For comparison of elevations between sites, the absolute elevation of the highest living *Porites* microatoll is assumed to be similar at each site. We conservatively estimate the maxi-

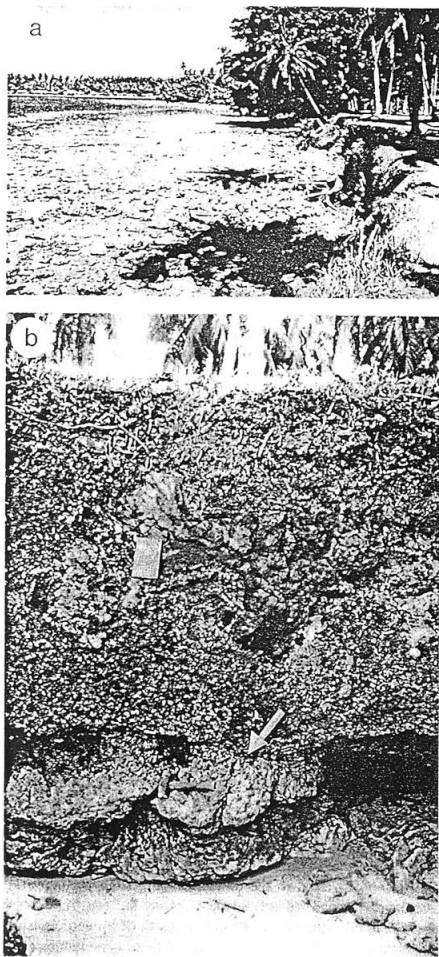


Figure 3. (a) The present-day reef flat and the lower coastal cliff and terrace at Jais Aben. Note the evidence of active erosion of the cliff, which, combined with the relatively narrow reef flat (~30–40 m wide), lends support to the concept of a major tectonic uplift event within the past few centuries. (b) Lower coastal cliff at Jais Aben. Massive *Porites* coral microatolls of 1–2 m diameter (e.g., under hammer) are abundant in a layer near the base of the cliff. The tops of these corals (e.g., arrow) form a distinctive boundary which is present throughout the field area. This boundary indicates the former position of sea level. Above the massive coral layer the cliff comprises a mixed branching and massive coral assemblage which indicates a rapid rise in relative sea level. Subsequent uplift has resulted in the present-day subaerial exposure of these reefs. (The hammer is 240 mm long.)

mum likely error associated with this assumption to be  $\pm 0.25$  m.

Observations were made on the composition and structure of corals within the exposed cliffs. In particular, the occurrence of massive corals with a flat-topped or more complex microatoll morphology was documented to help elucidate the past relative sea level history of the area. Samples of in situ massive *Porites*, *Goniastrea aspera* and *Favia fava* corals were collected for U/Th and  $^{14}\text{C}$  dating. These coral samples were inspected under binocular microscope for evidence of recrystallization, and only those which appeared pristine were taken for dating. Samples collected for U/Th dating were further examined by quantitative X-ray diffraction to assess mineralogy, and only corals with <1% calcite were subsequently dated.

U/Th dating of the coral samples was achieved at Edinburgh University by alpha spectrometry using silicon surface barrier detectors, following the methodology of Veeh [1966]. Complete dissolution of 2–5 g of sample was followed by ion exchange separation and electrolysis to prepare separate U and Th sources. A mixed spike of  $^{232}\text{U}$  and  $^{228}\text{Th}$  was used to determine isotopic activities of the  $^{232}\text{Th}$ ,  $^{230}\text{Th}$ ,  $^{238}\text{U}$ , and  $^{234}\text{U}$  isotopes. Samples were counted for 2–10 days using exclusive U and Th isotope detectors to minimize the alpha recoil contamination. Background count measurements were performed under identical conditions prior to the counting of each sample. U/Th ages are expressed as years B.P. (before 1950) with 2 sigma errors based only on counting statistics.

Measurements for  $^{14}\text{C}$  dating were made by Beta Analytic Inc.  $^{14}\text{C}$  ages were corrected to estimates of calendar years B.P. following Stuiver and Braziunas [1993] and Stuiver and Reimer [1993], by first correcting for  $\delta^{13}\text{C}$ , then assuming  $\Delta R$  (the difference in reservoir age of the local region compared to the model ocean) to be zero. That is, the dates have been corrected for a marine reservoir effect which averages about 400 years. Although no known-age samples were dated in this study, Chappell and Polach [1976] reported apparent ages of 535 and 270 years for two living specimens (clam and coral) from Huon Peninsula reefs. The average of these values is almost exactly the reservoir correction generated by the Stuiver and Reimer [1993] model, supporting its application in this case. Two sigma ranges for dates are based on counting statistics alone and, therefore, do not take into account any additional uncertainty on reservoir age correction. Previous studies have indicated that coral  $^{14}\text{C}$  ages corrected in this way to calendar years B.P. are close to coral U/Th ages [Bard et al., 1990, 1993]. Therefore, from this point forward, corrected  $^{14}\text{C}$  ages and U/Th ages are both referred to as "calendar years B.P.."

## 5. Results

At all of the coastal sites investigated (i.e., all sites except the Jais Aben access road), a distinct sedimentary discontinuity forms a boundary toward the base of the lower cliff. Beneath this boundary, large (1–2 m lateral diameter) massive *Porites* corals are abundant, and many of these have a microatoll morphology. The flat tops of these corals occur at, and locally define, the boundary. No individual coral colonies (branching or massive) were observed to grow through the boundary at any of the sites, and the boundary itself is rela-

tively flat-lying, with an undulating relief of <math><0.5\text{ m}</math> over lateral distances of at least 200 m. The largest (2 m diameter) flat-topped microatolls indicate relatively stable sea level ( $\pm 0.1\text{ m}</math>) over a period of  $\sim 100$  years during their growth (based on average coral growth rates of  $\sim 10\text{ mm/yr}</math>). In addition, the widespread occurrence of this boundary throughout the area suggests that the period of relative sea level stability may have lasted for considerably longer than 100 years. That is, not all the corals necessarily lived at exactly the same time; some may have died and become embedded in an intertidal reef flat before (younger) microatolls formed at the same elevation on an adjacent, prograding, reef crest.$$

Above the distinctive layer of microatolls the reefal deposits contain a higher proportion of branching coral (mainly *Acropora*; as in situ thickets and as rubble), less abundant massive corals (*Porites* and faviids), and interstitial sediment consisting of coral and mollusc-rich sands and gravels. Some of the branching coral material immediately above the boundary forms 0.5-1.0 m high upright thickets implying in situ growth into  $>1.0\text{ m}</math> water depth. No massive coral microatolls were observed in the 1-1.5 m immediately above the boundary, but microatolls do occur in the uppermost 0.5-1.0$

m of the cliff. These relationships are illustrated in Figure 4.

At the three surveyed sites the highest parts of the boundary between the flat-topped massive coral layer below and the mixed branching and massive coral assemblage above occur at an elevation between +1.4 m and +1.2 m with respect to nearby living reef crest *Porites* microatolls. Visual estimates indicate a similar elevation for the other six sites. The elevation of the top of the lower coastal cliff ranges from +3.0 m at the mainland sites down to about +2.7 m on some of the islands. The top of the second, upper, cliff is more variable in elevation but reaches up to +5.8 m. Although poorly exposed, the nature of the mixed branching and massive coral assemblage within this upper cliff (including *G. aspera*, which is a common intertidal and shallow subtidal species) is suggestive of growth in relatively shallow water, probably  $<5\text{ m}</math> deep. Farther inland, at the Jais Aben access road site, one coral sample was collected for  $^{14}\text{C}$  dating from a bank at about +2.2 m elevation. Local high points in the same formation reach up to about +2.7 m elevation. Once again, the coral assemblages within this formation (including *F. favius* and *G. aspera*) are suggestive of growth in relatively shallow water.$

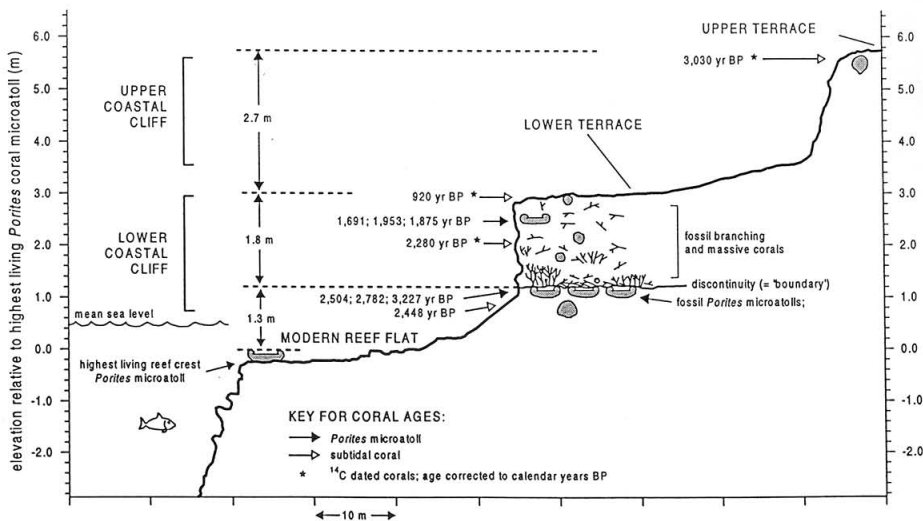


Figure 4. Diagram illustrating the field and age relationships observed in the coastal cliffs at the sites investigated in the Madang lagoon. The lower coastal cliff, with the distinct boundary toward its base, is present at all of the coastal sites. The upper coastal cliff was only seen to be well developed at Jais Aben and at Mililat Harbour. All ages are calendar years B.P. and are based on either U/Th ages or on corrected  $^{14}\text{C}$  ages (Tables 1 and 2).

Table 1. U and Th Isotopic Composition and Age Data for Massive *Porites* Corals From the Lower Coastal Cliff, Madang Lagoon

Coral Label	Location	Below or Above Boundary in Lower Cliff	Elevation With Respect to Living <i>Porites</i> Microatoll, m	$^{234}\text{U}/^{238}\text{U}$ (Activity Ratio)	$^{230}\text{Th}/^{232}\text{Th}$ (Activity Ratio)	$^{230}\text{Th}/^{234}\text{U}$ (Activity Ratio)	$^{232}\text{Th}$ , dpm/g	U, ppm	U/Th Age, years B.P.	Mean Age for Coral, years B.P.
M92-JA-FC5*	Jais Aben	below	+1.02	1.14 ± 0.03 1.14 ± 0.03	6.88 ± 2.78 4.02 ± 1.20	0.03 ± 0.00 0.03 ± 0.00	0.01 0.01	2.45 2.47	3409 ± 425 3045 ± 392	3227 ± 425
M92-JA-FC4 <sup>b</sup>	Jais Aben	below	+1.12	1.12 ± 0.03	7.15 ± 3.30	0.03 ± 0.00	0.01	2.46	2780 ± 409	2782 ± 409
M94-W-FC8 <sup>c</sup>	Wongat Island	below	+0.70	1.13 ± 0.02 1.14 ± 0.02	10.44 ± 2.87 13.22 ± 3.91	0.02 ± 0.00 0.02 ± 0.00	0.00 0.00	2.49 2.78	2517 ± 192 2490 ± 195	2504 ± 195
M93-T-FC1 <sup>d</sup>	Tabat Island	below	+0.25	1.19 ± 0.02 1.14 ± 0.02 1.18 ± 0.02 1.11 ± 0.02	61.80 ± 45.85 155.84 ± 326.54 40.12 ± 20.32 34.89 ± 24.47	0.02 ± 0.00 0.02 ± 0.00 0.02 ± 0.00 0.02 ± 0.00	0.00 0.00 0.00 0.00	2.55 2.58 2.48 2.57	2473 ± 195 2453 ± 206 2502 ± 210 2366 ± 217	2448 ± 217
M92-JA-FC1 <sup>e</sup>	Jais Aben	above	+2.50	1.13 ± 0.02 1.12 ± 0.02	2.80 ± 0.77 4.51 ± 1.15	0.01 ± 0.00 0.02 ± 0.00	0.01 0.01	2.99 2.97	1615 ± 269 2135 ± 267	1875 ± 269
M92-JA-FC3 <sup>f</sup>	Jais Aben	above	+2.50	1.09 ± 0.02 1.16 ± 0.02	5.63 ± 3.07 4.24 ± 1.26	0.02 ± 0.00 0.02 ± 0.00	0.01 0.01	2.72 2.61	2038 ± 310 1868 ± 231	1953 ± 310
M94-JA-FC1 <sup>g</sup>	Jais Aben	above	+2.57	1.13 ± 0.01 1.16 ± 0.01 1.13 ± 0.01 1.14 ± 0.01	6.70 ± 0.94 9.02 ± 1.40 6.36 ± 0.94 5.62 ± 0.78	0.02 ± 0.00 0.02 ± 0.00 0.01 ± 0.00 0.02 ± 0.00	0.01 0.00 0.01 0.01	2.94 2.85 2.89 2.86	1742 ± 91 1690 ± 90 1576 ± 88 1756 ± 93	1691 ± 91

Elevations are for the top of the dated coral and are relative to the top of the highest living *Porites* coral microatoll on the reef front/reef crest at each site. At Jais Aben, leveling determined this highest living *Porites* microatoll to be -0.49 m with respect to mean sea level as defined by Australian Commonwealth Scientific and Industrial Research Organisation (CSIRO) for the nearby tide gauge. Indicated errors for isotope ratios and individual ages are 2 sigma limits based on counting statistics. Mean ages for each coral are calculated as the mean of all replicate ages, and the indicated errors are conservatively taken as the largest 2 sigma error for individual samples from the coral. All corals were in growth position.

<sup>a</sup>A 2 m horizontal diameter, 0.7 m thick *Porites* microatoll in lower part of cliff. Top of microatoll defines the boundary as described in the main text.

<sup>b</sup>A 1.5 m horizontal diameter, 0.6 m thick *Porites* microatoll in lower part of cliff. Top of microatoll defines the boundary.

<sup>c</sup>A 2 m horizontal diameter, 1.0 m thick *Porites* microatoll in lower part of cliff. Top of microatoll defines boundary.

<sup>d</sup>A 2 m horizontal diameter, 0.9 m thick, round-topped *Porites* coral exposed in raised reef pavement adjacent to base of cliff, a few tens of centimeters below the elevation of the boundary.

<sup>e</sup>A 1.5 m horizontal diameter, 0.4 m thick *Porites* microatoll in upper part of cliff. Top of microatoll is -0.5 m below top of cliff.

<sup>f</sup>A 1.2 m horizontal diameter, 0.8 m thick massive *Porites* microatoll in upper part of cliff. Top of microatoll is -0.5 m below top of cliff.

<sup>g</sup>A 1.0 m horizontal diameter, 1.0 m thick massive flat-topped *Porites* in upper part of cliff. Top of coral is -0.4 m below top of cliff.

Table 2. Age and  $\delta^{13}\text{C}$  Data for Coral Samples Dated by  $^{14}\text{C}$ 

Sample (Lab No.)	Location	Position in Cliffs	Elevation With Respect to Living <i>Porites</i> Microatoll, m	$^{14}\text{C}$ Age, Not Isotope-Corrected, years B.P.	$\delta^{13}\text{C}$ , ‰ PDB	Calendar Age and 2 Sigma Range, years B.P.
CRI-01 <sup>a</sup> (Beta-29854)	Wongat Island	lower coastal cliff	- +2.0	2170 ± 80	+0.6	2280 (2420-2036)
CRI-02 <sup>b</sup> (Beta-29855)	Jais Aben	top upper coastal terrace	- +5.5	2820 ± 90	+0.6	3030 (3276-2786)
CRI-03 <sup>c</sup> (Beta-29856)	Jais Aben access road	inland	- +2.2	4710 ± 100	-0.8	5,450 (5646-5241)
CRI-05 <sup>d</sup> (Beta-29857)	Jais Aben	top lower coastal terrace	- +3.0	970 ± 70	+ 0.4	920 (1054-756)

Calendar ages estimated following *Stuiver and Braziunas* [1993] and *Stuiver and Reimer* [1993], assuming  $\Delta R$  (difference in reservoir age of local region compared to model ocean) to be zero. Two sigma ranges for calendar ages are based on counting statistics only. All samples appeared to be in growth position. Radiocarbon and  $\delta^{13}\text{C}$  measurements are by Beta Analytic Inc.

<sup>a</sup>A 1 m diameter *Goniastrea aspera* colony from seaward side of Wongat Island, 15 m inland from low-tide line.

<sup>b</sup>A 0.3 m diameter *G. aspera* colony from seaward edge of upper coastal terrace.

<sup>c</sup>A 0.25 m diameter half-hemispherical *Favia fava* colony atop a columnar base (total height 0.35 m) growing out and upward from the side of a near-vertical bank. Sample is located about 1.5 km inland from main coast, 150 m east of highway along Jais Aben access road. Location is 1.7 m above local tidal stream; top of bank is ~2 m above sea level, and local high points are ~2.5 m above sea level.

<sup>d</sup>A 0.4 m diameter *G. aspera* colony excavated from seaward edge of lower coastal terrace.

U/Th dating of four massive *Porites* corals from beneath the boundary in the lower cliff yielded ages ranging from  $3227 \pm 425$  to  $2448 \pm 217$  calendar years B.P. Five massive corals from above the boundary in the lower cliff yielded ages ranging from 2280 (2420-2036) to 920 (1054-756) calendar years B.P. A massive coral from the top of the upper cliff dated at 3030 (3276-2786) calendar years BP, and a coral from the inland Jais Aben access road site yielded an age of 5450 calendar years B.P. Full results of the U/Th and  $^{14}\text{C}$  dating programs are presented in Tables 1 and 2, respectively.

## 6. Discussion and Conclusions

All of the raised reefs investigated formed since ~5500 calendar years B.P. Estimates of relative sea level for Madang based on the Ice-4G model of the glacial isostatic adjustment process (as recently described by *Peltier* [1998]) indicate a falling sea level over this timeframe. Specifically, relative eustatic sea level is estimated by the model to have been about +4.5 m at 5000 years B.P., falling to about +2.1 m at 3000 years B.P. and +0.9 m at 1000 years B.P. (Figure 5). Rapid changes in observed relative sea level at Madang which deviate significantly from this modeled estimate of gradually falling eustatic sea level are likely to reflect vertical motion of the land due to tectonic activity. This assumption is made throughout the rest of the discussion.

Figure 5 presents a plot of age versus elevation of the dated corals and a relative sea level curve labeled with uplift and subsidence events. For comparison, and to aid with reconstruction of trends in relative sea level during periods of inferred tectonic stability, the estimated relative sea level for Madang due to glacial isostatic adjustment [*Peltier*, 1998] is also indicated. Although the current study focuses on evidence from the two coastal cliffs, the starting point for this discussion of vertical movements of the land is the single date of ~5500 calendar years B.P. from a coral at +2.2 m elevation at the inland Jais Aben access road site. Unfortunately, it is

not possible for us to accurately constrain relative sea level for this period since no coral microatolls were observed in this exposure. Nonetheless, the coral assemblages are suggestive of growth in relatively shallow water, which leads us to speculate that relative sea-level was probably between about 3 and 6 m above present.

The single  $^{14}\text{C}$ -based age for the top of the upper terrace is indistinguishable from two of the four U/Th ages for corals from beneath the boundary at the base of the lower coastal cliff. Clearly, given the height difference and the fact that the dated corals beneath the boundary are microatolls, all of these corals cannot be truly of the same age. For the corals at the base of the lower cliff to be older than the coral at the top of the upper terrace there would have had to have been a relative sea level rise of  $\geq 4.5$  m about 3000 calendar years B.P. with subsequent vertical growth of corals up to the new level within a period of two or three hundred years (i.e., at rates of several tens of mm/yr) followed by a drop in relative sea level of the same amount (i.e.  $\geq 4.5$  m) around 2700 calendar years B.P. We believe this to be extremely unlikely. Instead, we suggest that the coral at the top of the upper terrace is older than all the corals dated at the base of the lower terrace and that the relationships may be explained by a single drop in relative sea level of  $\geq 4.5$  m caused by a coseismic uplift event ~3000 calendar years BP with subsequent growth of coral microatolls up to the new lower relative sea level. These corals grew from foundations consisting of either the former forereef deposits of the upper terrace reef or an erosional platform cut back into the former upper terrace reef. In this scenario the period between ~5500 and 3000 calendar years B.P. may have been characterised by net tectonic subsidence, either gradually or as one (or more) rapid events.

The mixed branching and massive coral sequence on top of the boundary in the lower cliff indicates a relative rise in sea level, and hence an inferred tectonic subsidence of  $>2.0$  m. Since no corals were observed to have grown up through the boundary, it is inferred that in the sections examined, these



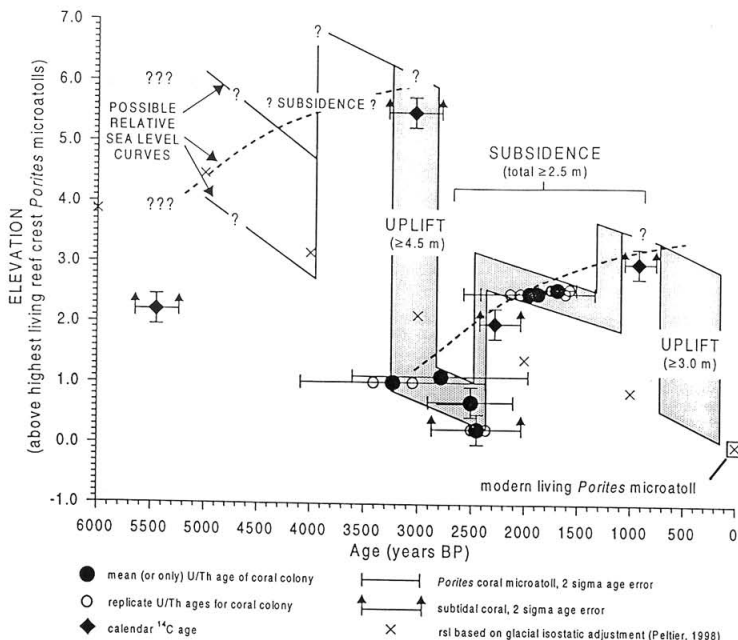


Figure 5. Plot of age (in calendar years B.P.) against elevation of dated corals discussed in this study. Two possible relative sea level curves are illustrated: The solid line with shaded regions of uncertainty illustrates a scenario where subsidence occurs as discrete coseismic events; the dashed line indicates a scenario where subsidence is a result of recovery following uplift. Consideration of the available evidence suggests that the coseismic subsidence scenario is the most probable. The crosses indicate estimated relative sea level for Madang based on the Ice-4G model of glacial isostatic rebound as described by Peltier [1998]; these model output are used to estimate actual relative sea level change (solid line) during periods of inferred tectonic stability. See text for further discussion. Age estimates have 2 sigma error bars based on counting statistics only; for the U/Th ages the errors associated with single age determinations are shown bracketing the mean colony age. Vertical (height) error bars for two U/Th dated corals are based on an estimate of the likely maximum error when these corals from Wongat Island are compared to the rest of the U-series-dated corals from Jais Aben (due to potential errors associated with using the height of the highest living local *Porites* microatoll as an absolute datum). Vertical error bars for the <sup>14</sup>C dated corals are estimates of the likely maximum error when these corals (which were not surveyed with leveling equipment) are compared to all other corals.

corals were most probably already dead and embedded in a reef flat at the time of the subsidence. The presence of thickets of in situ branching *Acropora* up to 1 m in height growing directly above the boundary is suggestive of instantaneous (or extremely rapid, e.g., >50 mm/yr) rise in sea level to accommodate the unrestricted vertical growth of these corals. A rapid rise in sea level is further supported by the absence of any corals with microatoll form in the 1–1.5 m above the boundary. These features of the internal structure and composition of the reef deposits, combined with the results of the dating, point to a subsidence event of 1.5–2.0 m about 2400 calendar years B.P.

Several *Porites* coral microatolls were observed and sampled from ~1.5 m above the boundary in the lower terrace.

All but one of these had relatively flat tops indicative of relatively stable sea level during growth. The exception was a colony which had clearly tilted during its life. Therefore there may have been a period of relative sea level stability ~2000 calendar years B.P., followed by another pulse of ≥0.5 m subsidence ~1200 years B.P. to generate the space for the accumulation of the upper 0.5 m of the lower terrace.

The present elevation of the top of the lower cliff indicates a more recent relative sea level fall, and hence inferred net tectonic uplift, of ≥3 m (including any postseismic submergence or emergence). The dating results suggest that this uplift occurred within the past 1000 years. Consideration of the rate of erosion of these Holocene cliffs and the width of the present-day reef flats lends support to the concept of a



major uplift event in the recent past. The average width of the reef flat at the Jais Aben site is approximately 40 m (Figures 3 and 4). This width indicates the maximum amount of lateral erosion that can have occurred since the uplift event. Anecdotal evidence from local villagers and consideration of the spacing and loss due to undercutting of coconut palms planted after World War 2 (Figure 3) suggests that the cliff has cut back on the order of 5–10 m over the past 30–40 years, that is, at an average rate of  $\sim 0.1$ – $0.3$  m/yr. This compares favorably with our own visual observation of erosion at this site over the period 1988–1996. Although these observations and estimates should not be regarded as reliable quantitative measures of the longer-term erosion of the cliffs, they do suggest that the major uplift event may have occurred within the past few centuries. Indeed, the Russian naturalist *Miklouf(c)ho-Maclay* [1884, 1975], who made the first systematic natural history observations of the Madang area in the 1870s, reported on the frequency and intensity of earthquakes and on the very considerable fear that the indigenous people had of earthquakes. This may imply that catastrophic earthquakes had occurred within collective human memory of the 1870s.

The two uplift events described here are similar in amplitude to late Quaternary events on the Huon Peninsula which were inferred to be coseismic in origin and to have a recurrence interval of 1000–1200 years [Chappell *et al.*, 1996a; Ota *et al.*, 1993]. Chappell *et al.* [1996a] concluded that these 1.4-m-scale events did not appear to be part of a continuum of uplift magnitudes on the Huon Peninsula, but instead appeared to belong to a separate class of events. They also pointed out that uplifts of 1–4 m were 10–40 times greater than the uplift at the Huon Peninsula caused by an earthquake in May 1992 [Pandolfi *et al.*, 1994]. A coseismic origin also seems probable for the Madang uplifts, either as single catastrophic events or, conceivably, as accumulations of smaller events over short periods of greatly increased seismic activity.

In contrast to the uplift events the intermittent tectonic subsidence at Madang does not appear to have an analogue on the Huon Peninsula. The Madang subsidence could be the result of rupture on a nearby fault, or it could be related to either the pulling down of the upper plate in a preseismic locked subduction zone or postseismic relaxation following a subduction zone earthquake. If subsidence is related to rupture on a fault, it is most likely that the region is on the hanging wall of one reverse fault, which leads to uplift, but on the footwall of another, which leads to subsidence. Alternating uplift and subsidence would then be the result of alternating failure on these two faults. This seems entirely plausible, and perhaps likely, with identification of NW-SE striking reverse faults in the Adelbert Range that trend toward the Madang lagoon and possible NE striking cross faults in Astrolabe Bay (Figure 1).

We prefer the interpretation that subsidence at Madang has been coseismic in response to nearby fault rupture. The alternative explanation, that subsidence is either the pulling down of the upper plate in a preseismic locked subduction zone or postseismic relaxation following a subduction zone earthquake [Thatcher and Rundle, 1979; Savage, 1983; Sato and Matsuura, 1993; Cohen, 1994], is not supported by the observed relative sea level stability for a hundred, and perhaps several hundred, years after the inferred major uplift event at  $\sim 3000$  calendar years B.P. or by the inferred instantaneous or very rapid subsidence around 2400 calendar years B.P. However, the northern Papua New Guinea collision zone is char-

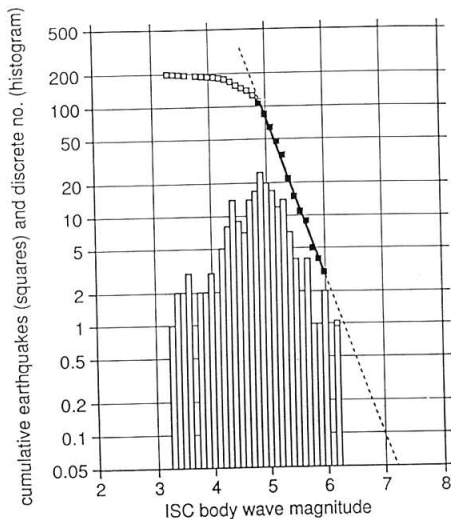


Figure 6. Plots of discrete (histogram) and cumulative (square symbols) number of earthquakes binned in intervals of 0.1 units of International Seismological Centre (ISC) body wave magnitude  $m_b$  in a 100 km radius region centered on Madang for the period 1964–1993. A least squares regression to the linear portion of the curve (solid squares) is shown, and gives a  $b$  value of 1.48. Extrapolation of this  $b$  value to magnitude 7.0 yields an estimate of 0.1 events in 30 years, or a return time of 300 years.

acterized by continental crust in both plates; therefore the deformation signal associated with large-earthquake cycles may not be well characterized by models proposed for subduction of oceanic crust, a point emphasized by Cohen (1994). Therefore, we must be tentative in drawing tectonic implications from our observations.

We can use present-day seismicity reported in the Catalogue of the International Seismological Centre (ISC) to estimate return times for earthquakes capable of generating meter-scale coseismic displacements. Figure 6 shows cumulative and discrete body wave magnitude ( $m_b$ ) versus frequency plots for shallow (ISC depth  $< 60$  km) earthquakes within 100 km of Madang for the period 1964–1993. This 100 km radius is the region within which a large (say,  $m_b$  7.0 or greater) thrust earthquake may be expected to significantly influence vertical displacement in our field area. The familiar Gutenberg-Richter linear relationship is observed in the cumulative data between  $m_b$  4.5 and  $m_b$  6.0. Below this range the data set is inferred to be incomplete, and the nonlinearity above  $m_b$  6.0 implies a magnitude limit above which either earthquakes do not occur in this region or our time period is insufficient (causing either a deficit or excess at large magnitudes; see below). The cumulative data between these magnitude limits give a seismic  $b$  value of 1.48.

We know that earthquakes of  $m_b$  7.0 have occurred in northern Papua New Guinea, although there is no seismic

evidence of larger magnitudes. Since seismic moment, and hence displacement, is dominated by the largest-magnitude earthquakes in a region, we choose to estimate the return time of an earthquake of  $m_b$  7.0. Extrapolation of our  $b$  value line to  $m_b$  7.0 infers 0.1 earthquakes of this magnitude or above in 30 years, giving a return time of 300 years. It is well known that ISC magnitudes are subject to various sources of bias. However, use of maximum-likelihood body wave magnitudes computed by the method of *Lilwall* [1987] to reduce these biases yields a similar return time.

This estimation of return time for seismic events capable of producing meter-scale uplift and subsidence necessarily embodies several assumptions, each of which is open to conjecture. The most important of these are that the maximum body wave magnitude achieved in this region is  $\geq 7.0$  and that thrust earthquakes dominate the seismicity in the 100 km radius zone of interest. Furthermore, the seismic  $b$  value of 1.48 is high, which may imply a deficit of large-magnitude earthquakes during the sampling interval. If the true  $b$  value is smaller (i.e., in the usual range of 0.8–1.2), then our return time estimate of 300 years is too high. On the other hand, it may be that a magnitude greater than  $m_b$  7.0 is required to effect meter-scale uplift in this type of tectonic setting, in which case our estimated return time is too short. For example, *Berryman* [1996] used dislocation modelling of the geometry of the thrust earthquake zone under the Huon Peninsula to deduce that magnitude  $m_b$  7.9–8.3 earthquakes were required to produce 1–4 m uplift events. Despite these uncertainties the seismic evidence is entirely consistent with the proposed coseismic origin for the relative sea level variations reported here.

Recognition of intermittent subsidence has several wider implications. First, it may help explain the apparent discrepancy between the rapid late Holocene net uplift rates (e.g.,  $>1$  mm/yr) and the lack of an elevated flight of late Quaternary raised reef terraces analogous in extent and elevation to those exposed on the Huon Peninsula. That is, the tectonic setting of Madang appears to be such that intermittent subsidence events partially offset the effects of uplift events. Second, the potential for coseismic subsidence implies a greater latent hazard to coastal communities in the region than might be assumed from simple consideration of the evidence of longer-term net tectonic uplift. Third, the study illustrates how detailed analysis of raised reef deposits may be used to reconstruct rapid and alternating relative sea level changes with a temporal resolution of a few centuries over thousands of years. In situations of stable eustatic sea level these may be interpreted in terms of tectonic displacements, whereas in regions of tectonic stability they may be interpreted in terms of eustatic sea level change. Finally, in a broader geological context the Madang reefs illustrate that intermittent reversal of a general tectonic trend can exert a profound control on the sedimentary architecture, evolution, and, therefore, facies of the accumulating deposit.

**Acknowledgments.** This work was financially supported by the U.K. Natural Environment Research Council grants GR3 09961 and GR3 8475 (A.W.T. and G.B.S.), U.S. Department of Energy Lawrence Livermore National Laboratory contract W-7405-Eng-48 (R.W.B.), NSF grant EAR 84-08001 (J.H.L.) and the Christensen Research Institute (Fellowships to A.W.T., R.W.B., D.G.F. and J.H.L.). We thank Christensen Research Institute for logistic support and the local landowners for access to their land and for help in the field. Tim Fletcher, T. Frohm, John Mizeu, Jim Smith, and Meri-

wether Wilson are gratefully acknowledged for field assistance, and J. Darr and A. Bulcock are acknowledged for helpful information on local geology. Ken Ridgeway of CSIRO, Hobart, kindly provided information on the Madang tide gauge elevation. Dick Peltier generously provided us with output from the Ice-4G model of relative sea level run for Madang. This manuscript benefitted significantly from the suggestions of Kerry Sieh, Yehuda Bock, and another, anonymous, reviewer. Finally, thanks to John Chappell for his enthusiasm for sharing ideas.

## References

- Abbott, L.D., Neogene tectonic reconstruction of the Adelbert-Finisterre-New Britain collision, northern Papua New Guinea, *J. Southeast Asian Earth Sci.*, **11**, 33–51, 1995.
- Abbott, L.D., E.A. Silver, and J. Galewsky, Structural evolution of a modern arc-continent collision in Papua New Guinea, *Tectonics*, **13**, 1007–1034, 1994.
- Abers, G.A., and R. McCaffrey, Active arc-continent collision: Earthquakes, gravity anomalies, and fault kinematics in the Huon-Finisterre collision zone, Papua New Guinea, *Tectonics*, **13**, 227–245, 1994.
- Bard, E., B. Hamelin, R.G. Fairbanks, and A. Zindler, Calibration of  $^{14}\text{C}$  timescale over the past 30,000 years using mass spectrometric U-Th ages from Barbados corals, *Nature*, **345**, 791–794, 1990.
- Bard, E., M. Arnold, R.G. Fairbanks, and B. Hamelin,  $^{230}\text{Th}$ - $^{234}\text{U}$  and  $^{14}\text{C}$  ages obtained by mass spectrometry on corals, *Radiocarbon*, **35**, 191–199, 1993.
- Berryman, K.R., Mechanics of uplift of Quaternary marine terraces on Huon Peninsula, Papua New Guinea (abstract), *Eos Trans. AGU*, **77**(22), West. Pac. Geophys. Meet. Suppl., W119, 1996.
- Chappell, J., Geology of coral terraces, Huon Peninsula, Papua New Guinea: A study of Quaternary tectonic movements and sea-level changes, *Geol. Soc. Am. Bull.*, **85**, 553–570, 1974.
- Chappell, J., and H.A. Polach, Holocene sea-level change and coral-reef growth at Huon Peninsula, Papua New Guinea, *Geol. Soc. Am. Bull.*, **87**, 235–240, 1976.
- Chappell, J., and N.J. Shackleton, Oxygen isotopes and sea-level, *Nature*, **324**, 137–140, 1986.
- Chappell, J., Y. Ota, and K.R. Berryman, Late Quaternary co-seismic uplift history of Huon Peninsula, Papua New Guinea, *Quat. Sci. Rev.*, **15**, 7–22, 1996a.
- Chappell, J., A. Omura, T. Esat, M. McCulloch, J. Pandolfi, Y. Ota, and B. Pillans, Reconciliation of late Quaternary sea-levels derived from coral terraces at Huon Peninsula with deep sea oxygen isotope records, *Earth Planet. Sci. Lett.*, **141**, 227–236, 1996b.
- Cohen, S.C., Evaluation of the importance of model features for cyclic deformation due to dip-slip faulting, *Geophys. J. Int.*, **119**, 831–841, 1994.
- Everingham, I.B., Seismological report on the Madang earthquake of 31 October 1970 and aftershocks, *Rep. Bur. Miner. Resour. Geol. Geophys. Aust.*, **176**, 1975.
- Jaques, A.L., and G.P. Robinson, Bogia, Papua New Guinea, Geological Series, map and explanatory notes, 27 pp, scale 1:250,000, Geol. Surv. of Papua New Guinea, Port Moresby, 1980.
- Lilwall, R.C., Station threshold bias in short-period amplitude distance and station terms used to compute body-wave magnitudes  $m_b$ , *Geophys. J. R. Astron. Soc.*, **91**, 1127–1133, 1987.
- Miklouho-Maclay, N., On volcanic activity on the islands near the north-east coast of New Guinea and evidence of rising of the Maclay-coast in New Guinea, *Proc. Linn. Soc. N. S. W.*, **9**, 963–967, 1884.
- Miklouho-Maclay, N., New Guinea Diaries 1871–1883, Kristen Press, Madang, Papua New Guinea, 1975.
- Milson, J., Neogene thrust emplacement from a frontal arc in New Guinea, in *Thrust and Nappe Tectonics*, edited by K.R. McClay and N.J. Price, Geol. Soc. Spec. Pub., **9**, 417–426, 1981.
- Ota, Y., J. Chappell, R. Kelley, N. Yonekura, E. Matsumoto, T. Nishimura, and J. Head, Holocene reef terraces and co-seismic uplift of Huon Peninsula, Papua New Guinea, *Quat. Res.*, **40**, 177–188, 1993.
- Pandolfi, J.M., M.R. Best, and S.P. Murray, Co-seismic event of May 15, 1992, Huon Peninsula, Papua New Guinea: Comparison with Quaternary tectonic history, *Geology*, **22**, 239–240, 1994.

- Panzer, W., Junge Kuestenhebung im Bismark-Archipel und auf Neu-Guinea, *Z. Ges. Erdk. Berlin*, 1933, 175-190, 1933.
- Peltier, W.R., Postglacial variations in the level of the sea: Implications for climate dynamics and solid earth geophysics, *Rev. Geophys.*, 36, 603-689, 1998.
- Robinson, G.P., A.L. Jaques, and C.M. Brown, Madang, PNG, Geological Series with explanatory notes, sheet 3B/55-6, scale 1:250,000, Aust. Gov. Print. Serv., Canberra, 1976.
- Sato, R., and M. Matsu'ura, A kinematic model for evolution of island arc-trench systems, *Geophys. J. Int.*, 114, 512-530, 1993.
- Savage, J.C., A dislocation model of strain accumulation and release at a subduction zone, *J. Geophys. Res.*, 88, 4984-4996, 1983.
- Scoffin, T.P., and D.R. Stoddart, The nature and significance of microatolls, *Philos. Trans. R. Soc. London. Ser. B*, 284, 99-122, 1978.
- Stoddart, D.R., Catastrophic damage to coral reef communities by earthquake, *Nature*, 239, 51-52, 1972.
- Stuiver, M., and T.F. Braziunas, Modelling atmospheric  $^{14}\text{C}$  influences and  $^{14}\text{C}$  ages of marine samples to 10,000 BC, *Radiocarbon*, 35, 137-189, 1993.
- Stuiver, M., and P.J. Reimer, Extended  $^{14}\text{C}$  database and revised CALIB radiocarbon calibration program, *Radiocarbon*, 35, 215-230, 1993.
- Taylor, F.W., C. Frohlich, J. Lecolle, and M. Strecker, Analysis of partially emerged corals and reef terraces in the Central Vanuatu Arc: Comparison of contemporary coseismic and nonseismic with Quaternary vertical movements, *J. Geophys. Res.*, 92, 4905-4933, 1987.
- Thatcher, W., and J.B. Rundle, A model for the earthquake cycle in underthrust zones, *J. Geophys. Res.*, 84, 5540-5556, 1979.
- Tregoning, P., et al., Estimation of current plate motions in Papua New Guinea from Global Positioning System observations, *J. Geophys. Res.*, 103, 12,181-12,203, 1998.
- Veeh, H.H.,  $^{230}\text{Th}/^{234}\text{U}$  and  $^{234}\text{U}/^{238}\text{U}$  ages of Pleistocene high sea-level stand, *J. Geophys. Res.*, 71, 3379-3386, 1966.
- Zachariassen, J., K. Sieh, F.W. Taylor, R.L. Edwards, and W.S. Hantoro, Submergence and uplift associated with the giant 1933 Sumatran subduction earthquake: evidence from coral microatolls, *J. Geophys. Res.*, 104, 895-919, 1999.
- K. R. Berryman, Active Landscapes Section, Institute of Geological & Nuclear Sciences Ltd., Gracefield Research Centre, 69 Gracefield Road, P. O. Box 30-368, Lower Hutt, New Zealand.
- R. W. Buddemeier, Kansas Geological Survey, University of Kansas, 1930 Constant Avenue, Lawrence, KS 66047. (buddrw@kgs.ukans.edu)
- C. P. Chilcott, R. G. Pearce, and T. P. Scoffin, Department of Geology & Geophysics, Edinburgh EH9 3JW, Scotland, U. K.
- D. G. Fautin, Department of Systematics and Ecology, University of Kansas, Lawrence, KS 64044.
- M. Jebb, National Botanic Gardens, Glasnevin, Dublin 9, Ireland.
- J. H. Lipps, Museum of Paleontology and Department of Integrative Biology, University of California, Berkeley, CA 94720. (jlipps@ucmpl.berkeley.edu)
- G. B. Shimmiel, Dunstaffnage marine Laboratory, P. O. Box 3, Oban, Argyll PA34 4AD, Scotland, U. K. (gbs@wpo.nerc.ac.uk)
- A. W. Tudhope, Australian Institute of Marine Science, PMB 3, Townsville M.C., Queensland 4810. (sandy.tudhope@ed.ac.uk)

(Received September 23, 1998; revised April 23, 1999; accepted November 22, 1999)